CHEMISTRY OF MATERIALS

Article

pubs.acs.org/cm

Soft Nanotubes Acting as a Light-Harvesting Antenna System

Naohiro Kameta,* Kazuyuki Ishikawa, Mitsutoshi Masuda, Masumi Asakawa, and Toshimi Shimizu

Nanotube Research Center (NTRC), National Institute of Advanced Industrial Science and Technology (AIST), Tsukuba Central 5, 1-1-1 Higashi, Tsukuba, Ibaraki 305-8565, Japan

Supporting Information

ABSTRACT: Amphiphilic monomers, which were quantitatively synthesized from a dehydration reaction between a glycolipid and naphthalene-boronic acids, self-assembled in organic solvents to selectively form tape-like structures (nanotape) and tubular structures (nanotube) depending on the bond position of the boron atom in the naphthalene ring. The nanotube has a strong narrow fluorescence band attributable to the monomer species of the naphthalene group, whereas the nanotape has a weak broad fluorescence band at a relative longer wavelength region based on the excimer species of the naphthalene group. Light energy adsorbed by the naphthalene groups densely and regularly organized in the bilayer membrane wall of the nanotube was transferred, with high quantum efficiency, into anthracene as an acceptor encapsulated in the nanochannel. The supramolecular nanotube proved to be able to act as a light-harvesting antenna.

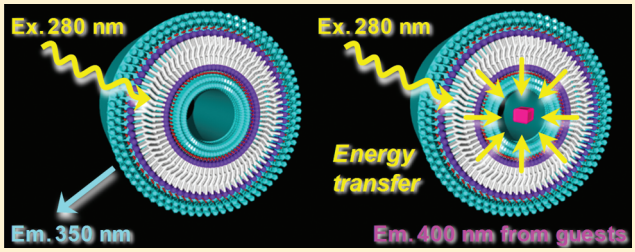

KEYWORDS: *self-assembly, supramolecular, nanotube, host−guest, energy transfer, light harvesting*

INTRODUCTION

Supramolecular and biomimetic chemistry have enabled us to construct artificial light-harvesting antenna systems, based on not only rod-like nanostructures[1] self-assembled from natural dyes such as chlorophyll and bacteriochlorophyll chromophores but also nanofibers, nanodisks (and those aggregated gels),[2−4] micelles, and vesicles[5] self-assembled from functionalized dyes. Tubular nanoarchitectures such as supramolecular nanotubes[6,7] and bionanotubes[8−10] including tabacco mosaic virus (TMV), which are formed by self-assembly of synthetic amphiphiles and biomacromolecules integrated with dye moieties, have also attracted much attention in the field of opto-electronic soft materials. The unique morphology having a completely one-dimensional structure with well-defined size dimensions and individually functionalized inner and outer surfaces,[11] which are different from the branching structure of nanofibers, should lead to a directional energy transfer and charge transfer. Actually, the embedded dye moieties within the wall of the above nanotubes have been known to show an excellent light-harvesting, photocatalytic, and electrical conduction abilities based on the efficient energy and charge transfers. The supramolecular nanotubes have nanochannels of 1−100 nm inner diameters which can act as hosts for small molecules, macromolecules, and nanoparticles.[12] However, the utilization of the nanochannels for the organization and alignment of the dye molecules has not been reported so far, while that of the inorganic porous channels in zeolites and mesoporous silica has been widely performed.[13] The supramolecular nanotubes have advantages in terms of the one-step formation process without template, controllable inner and outer diameters, functionalizable surfaces and membrane walls, and hierarchical organization into macro-scale soft materials such as gels and liquid crystals.[14]

Herein we present the newly designed and synthesized simple amphiphilic monomers **1** and **2** (Figure 1) quantitatively

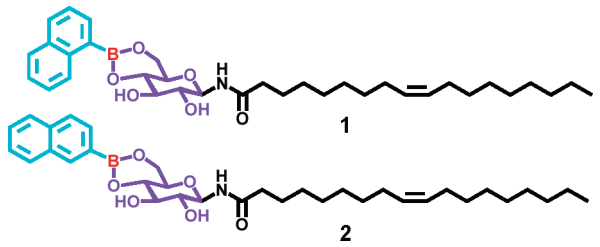

Figure 1. Amphiphilic monomers **1** and **2**.

obtained from dehydration reaction between a glycolipid and naphthalene-boronic acids (see Experimental Section and Supporting Information Figure S1), to selectively construct supramolecular nanotubes as a light-harvesting scaffold. We found that light energy adsorbed by the naphthalene groups densely organized within the bilayer membrane wall of the nanotube is transferred to anthracene encapsulated as an acceptor in the nanochannel, resulting in significant enhancement of emission from the anthracene. The confinement of the acceptor dye in the nanochannel composed of donor dyes leads to an effective energy transfer.

Received: October 10, 2011
Revised: December 2, 2011
Published: December 3, 2011

RESULTS AND DISCUSSION

Self-Assembly and Molecular Packing Analysis. The self-assembly experiment was performed as follows: Each synthetic amphiphile (1 mg) was dispersed in toluene (1 mL) under reflux conditions. The resultant hot solutions were gradually cooled to room temperature. The solution of **2** transformed into organogels having a strong fluorescence (Figure 2a), while

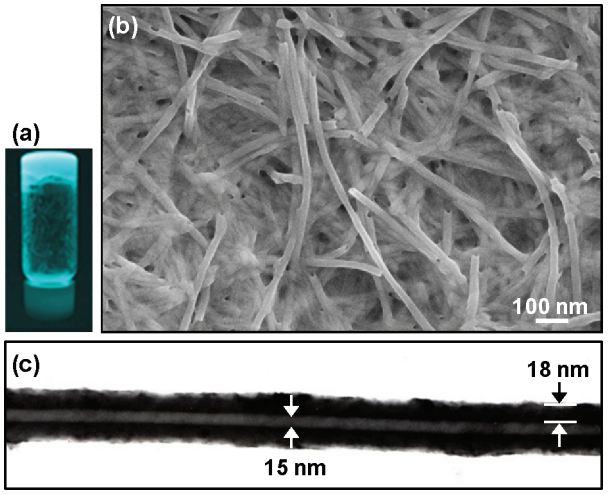

Figure 2. (a) Photograph of the nanotube organogel having a strong fluorescence. (b) SEM and (c) TEM images of the nanotubes self-assembled from **2**.

that of **1** gave precipitates. The critical gelator concentration of the nanotube organogel was 0.1 wt % in toluene. Valuable-temperature transmittance measurement for the nanotube organogel allowed us to estimate the gel-to-sol transition temperature (=65 °C). Scanning electron microscopic (SEM) and transmission electron microscopic (TEM) observation for the precipitate of **1** reveals the formation of tape-like structures in 20–100 nm widths (Supporting Information Figure S2). On the other hand, SEM observation for the xerogel of **2** displays well-defined open ends in the fibers, indicating that the self-assembled morphology in the organogel is identified as a tubular structure (Figure 2b). TEM observation clearly showed the uniform nanochannel with 15 nm inner diameter of the tubular structure (Figure 2c). Self-assembled morphologies strongly depended on the bond position of the boron atom in the naphthalene ring.

Powder X-ray diffraction (XRD) and infrared (IR) spectroscopic measurements afforded information about the molecular packing of the nanotape and nanotube (Figure 3). The XRD pattern gave a single diffraction peak in the small angle region. The membrane-stacking periodicities (d) of the nanotape and nanotube were 6.40 and 5.90 nm, respectively (Supporting Information Figure S3). Both d values were longer than that of a bilayer membrane (d = 4.53 nm), in which the glycolipid without naphthalene-boronic acids packs in interdigitated fashion.[15] The membrane thickness (18 nm) of the nanotube estimated from TEM image was closely related to three times the value of d, indicating that the nanotube consisted of stacking of three bilayer membranes. The IR spectra of the nanotape and nanotube showed two peaks at 731 and 720 cm^{-1} assignable to the $\gamma(CH_2)$ rocking vibration, suggesting that the lateral chain packing of the hydrocarbon chains of **1** and **2** is of an orthorhombic perpendicular type (Supporting Information

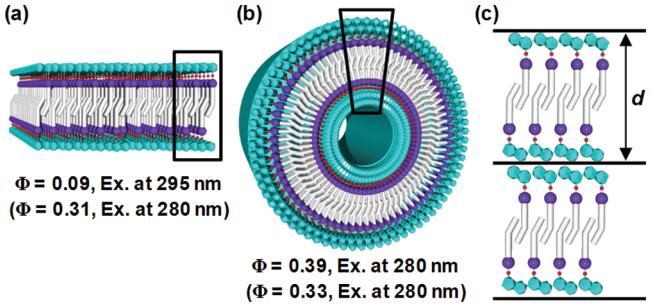

Figure 3. Schematic images of (a) the nanotape, (b) the nanotube, and (c) an interdigitated molecular packing within the bilayer membranes. Both assemblies are drawn as single-bilayer-membrane structures, although they are actually formed by stacking of the bilayer membranes. Fluorescence quantum yields of the nanotape and nanotube are also shown as well as those (in parentheses) of amphiphilic monomers **1** and **2**.

Figure S4a).[16] The subcell structure strongly supported the interdigitated molecular packing of **1** and **2** within the bilayer membrane. However, the intermolecular interaction within the bilayer membrane was remarkably different between the nanotape and nanotube. The hydrogen bond among **2** in the nanotube was stronger than that among **1** in the nanotape, since the amide I band of the nanotube was observed at lower wavenumber than that of the nanotape (Supporting Information Figure S4b). On the other hand, the $\pi-\pi$ stacking among **2** in the nanotube was weaker than that among **1** in the nanotape as mentioned below. As a result, we were able to independently form the nanotape and nanotube.

Absorption and Fluorescence Properties. The absorption band for the nanotape dispersed in $CHCl_3$ showed a red shift compared with that of **1** dissolved as a monomer in THF (Figure 4). On the other hand, the absorption band for the

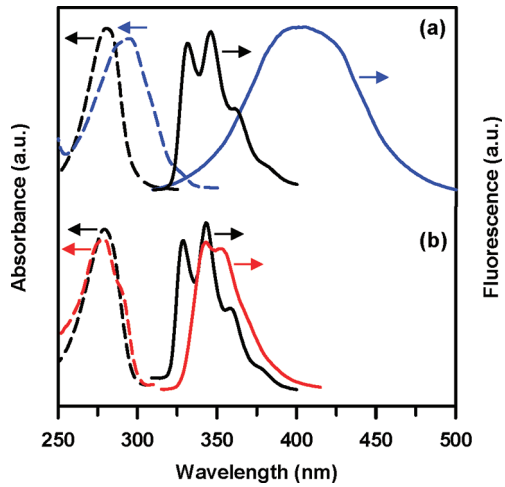

Figure 4. (a) Absorption spectra of the amphiphilic monomer **1** in THF (black dotted line) and the nanotape in $CHCl_3$ (blue dotted line). Fluorescence spectra of the amphiphilic monomer **1** in THF (black solid line) and the nanotape in $CHCl_3$ (blue solid line). (b) Absorption spectra of the amphiphilic monomer **2** in THF (black dotted line) and the nanotube in $CHCl_3$ (red dotted line). Fluorescence spectra of the amphiphilic monomer **2** in THF (black solid line) and the nanotube in $CHCl_3$ (red solid line).

nanotube dispersed in $CHCl_3$ had almost the same band as that of **2** dissolved as a monomer in THF. This means few interactions are present between the naphthalene groups within

dx.doi.org/10.1021/cm2030526 | Chem. Mater. 2012, 24, 209–214

the bilayer membranes of the nanotube in the ground state despite the dense molecular packing. The orientation of the naphthalene groups in the nanotube is obviously different from that of the naphthalene groups in the nanotape. Fluorescence bands for the nanotape and nanotube were obviously different from each other as expected from the absorption features. Namely, the nanotape exhibited a broad emission band in the 405 nm region based on the excimer species of the naphthalene groups, while the nanotube exhibited a relative narrow band at 350 nm based on the monomer species of the naphthalene groups even under the excited state (Figure 4).[17] Fluorescence quantum yield (Φ) of the nanotape was markedly lower than that of **1** as a monomer (Figure 3), which can be explained by the strong interaction in the excited state between the naphthalene groups, that is, solid-state quenching. In contrast, the Φ of the nanotube slightly increased from that of **2** as a monomer. The suppression and restriction of the intermolecular motion should promote an aggregation-induced fluorescence increment,[18] since the naphthalene groups were tightly fixed in the solid-state or crystalline-like bilayer membranes of the nanotube. In the nanotube system, the contribution of the aggregation-induced fluorescence increment will be larger than that of the solid-state quenching. In addition, the curved molecular packing to form the tubular morphology leads to isolate the naphthalene groups within the bilayer membrane wall and will inhibit the quenching process based on the formation of associated species in the ground and excited states. As a result, the nanotube showed the higher Φ comparing with the nanotape, although the absorption efficiency (ε = 5.4 × 10^3 M^{-1} cm^{-1}, 280 nm) of the nanotube was similar to that (ε = 7.0 × 10^3 M^{-1} cm^{-1}, 295 nm) of the nanotape.

Energy Transfer from the Nanotube to the Guest. Anthracene was used as a guest fluorescent acceptor, since the absorption band of anthracene overlapped well with the fluorescence band derived from the naphthalene moieties in the nanotube (Supporting Information Figure S5). Namely, the combination of both chromophores suits the induction of the energy transfer.[19] The encapsulation method is shown in the Experimental Section and Supporting Information Figures S6 and S7. We observed neither morphological change nor decomposition of the nanotubes after encapsulation of anthracene (Supporting Information Figure S8). The inner diameter and membrane thickness are similar to those of the nanotubes before encapsulation of anthracene. Fluorescence microscopic observation showed straight fluorescence images (Supporting Information Figure S9), indicating that high-axial ratio nanostructures, namely, the nanotubes encapsulating anthracene, stably exist in $CHCl_3$ solution without disassembly or molecular dispersion.

UV/vis absorption spectrum of the nanotube encapsulating anthracene as a guest acceptor in the nanochannel (10 mol % anthracene/naphthalene in the nanotube) reveals a large absorption band at a peak wavelength of 280 nm and a small absorption band at a peak wavelength of 350 nm (Supporting Information Figure S10). The two bands are assignable to the naphthalene groups densely packed in the nanotube membrane wall and the encapsulated anthracene in the nanochannel, respectively. Figure 5 shows the change in the fluorescence spectrum of the nanotube encapsulating anthracene in the nanochannel according to the concentration of the encapsulated anthracene (0−10 mol %). The fluorescence intensity of the naphthalene groups in the nanotube membrane wall at 350 nm decreased with increasing the concentration of the encapsulated

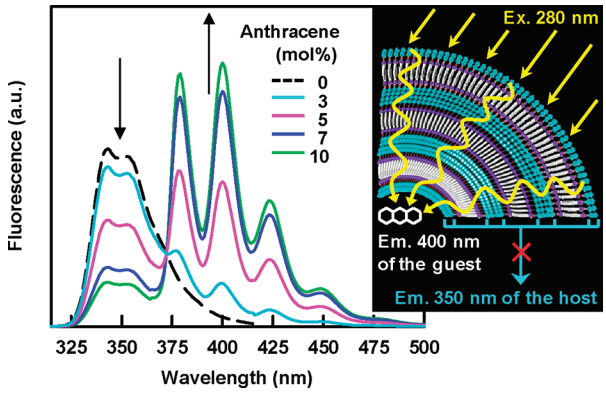

Figure 5. Fluorescence spectra of the nanotube encapsulating anthracene in the nanochannel (solid lines) and the only nanotube (dotted line) in $CHCl_3$. Schematic illustration of the energy transfer from the naphthalene groups densely organized within three bilayer membranes of the nanotube wall (the host) to the encapsulated anthracene (the guest) in the nanochannel.

anthracene. On the other hand, a fluorescence band of the anthracene newly appeared at 400 nm. This phenomenon was ascribable to an energy transfer from the naphthalene groups in the nanotube membrane wall to the encapsulated anthracene in the nanochannel, as emission upon direct excitation at 280 nm of the anthracene was negligible (<0.5%). Total Φ of two fluorescence components, which composed of the naphthalene groups in the nanotube membrane wall and the encapsulated anthracene in the nanochannel as the result of the energy transfer by the excitation at 280 nm, increased with increasing the concentration of the encapsulated anthracene (Figure 6a).

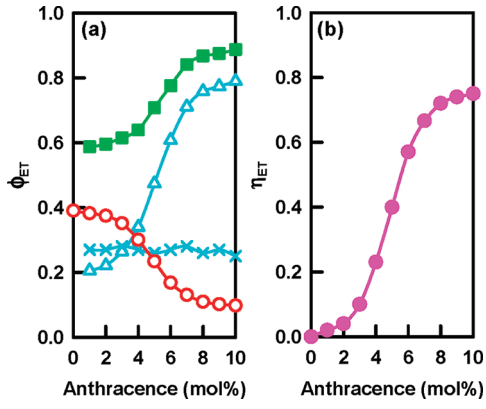

Figure 6. (a) Fluorescence quantum yield excited at 280 nm (○, △, ■) and 350 nm (×) as a function of anthracene concentration. From the naphthalene groups in the nanotube (○); from the encapsulated anthracence in the nanochannel (△, ×); total of ○ and △ (■). (b) Energy transfer efficiency as a function of anthracene concentration.

Such an orderly relationship between the total Φ and the anthracene concentration means that the effective energy transfer is unaccompanied with radiation and reabsorption pathways. The fluorescence of the encapsulated anthracene enhanced by the energy transfer under excitation at 280 nm is much higher than that of the anthracene by the direct excitation at 350 nm, representing that the nanotube functions as excellent light-harvesting antenna (Figure 6a, △, ×). Figure 7 shows the fluorescence decay profiles of the nanotube itself and nanotube encapsulating anthracene. The fluorescence decay of the

dx.doi.org/10.1021/cm2030526 | *Chem. Mater.* 2012, 24, 209−214

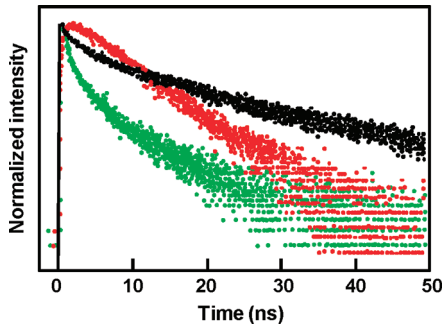

Figure 7. Fluorescence decay profiles of the nanotube 350 nm (black plots), and the nanotube encapsulating anthracene (10 mol %) monitored at 350 nm (green plots) and 425 nm (red plots) (excitation wavelength, 280 nm).

naphthalene groups in the nanotube was remarkably shortened after encapsulation of anthracene, accompanied with the fast rise in the decay profile by the fluorescence of anthracene. Therefore, the quenching process is attributable to the resonance energy transfer without a radiation process. Energy transfer efficiency ($\eta_{ET} = \Phi/\Phi_{init}$), which was estimated from the fluorescence quenching rate of the naphthalene groups in the nanotube membrane wall, reached 75% when the concentration of the encapsulated anthracene was 10 mol % (Figure 6b). The confinement of anthracene into the nanochannel with 15 nm inner diameter by the encapsulation should contribute to the high energy transfer efficiency. In fact, the energy transfer from the naphthalene groups in the nanotube membrane walls to free anthracene in bulk solution hardly occurred (Figure 8), reflecting

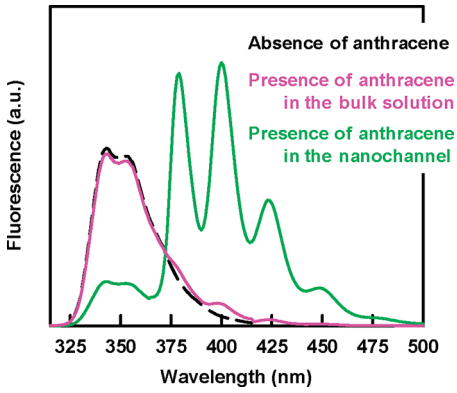

Figure 8. Fluorescence spectra of the nanotube in the presence (pink and green solid lines) and absence (black dotted line) of 10 mol % anthracence in $CHCl_3$ solution. The sample solution corresponding to the pink solid line was prepared by the mixing of the nanotube solution with anthracene. The nanochannel filled with $CHCl_3$ showed no encapsulation ability for anthracene based on lack of capillary force, in which anthracene exists as free in the bulk solution.[21]

that the donor–acceptor distance (Förster distance) is a most important factor for the η_{ET}

CONCLUSION

We have for the first time succeeded in the construction of the light-harvesting antenna system by combination of the supramolecular nanotube host as the fluorescent donor and guest dye molecules as the fluorescent acceptor. The energy transfer can be enhanced by appropriate selection and combination of aromatic groups in the nanotube membrane wall and guest acceptors in the nanochannel. Furthermore, control of the confinement effect based on the encapsulation of guest acceptors in the nanochannel will enable us to achieve the high energy transfer with 100% quantum efficiency,[20] which can be seen in the photosynthetic system in nature. Precise design of the amphiphilic monomers and introduction of other boronic acids bearing various aromatic rings such as thiophene, biphenyl, anthracene, and pyrene instead of the naphthalene used in the present study should be contributable to not only control of the confinement effect but also expand the absorption band region acceptable to sunlight irradiation. The present light-harvesting antenna system will open ways to develop optical and electronic soft materials applicable in photocatalysis and dye-sensitized solar cells.

EXPERIMENTAL SECTION

Synthesis of Amphiphilic Monomer 1. The synthetic scheme is in Supporting Information. The glycolipid, *N*-(9-*cis*-octadecenoyl)-*β*-D-glucopyranosylamine, was synthesized as reported previously. 1-Naphthaleneboronic acid was purchased from Tokyo Chemical Co. and was used in the following reaction without purification. Quantitative dehydration reaction between the glycolipid (0.44 g, 1 mmol) and 1-naphthaleneboronic acid (0.17 g, 1 mmol) in toluene was performed under the reflux condition equipped with a Dean–Stark apparatus. After 3 h, the solvent was completely removed by evaporation. The obtained residue was washed with anhydrous THF several times and was stored in vacuum desiccators. ^{1}H NMR (400 MHz, DMSO-d_6, δ): 8.39 (d, J = 9.1 Hz, 1H: NH), 8.02 (dd, J = 1.2 and 6.8 Hz, 1H: naphthalene), 7.98 (d, J = 8.0 Hz, 1H: naphthalene), 7.93–7.87 (m, 2H: naphthalene), 7.54–7.47 (m, 3H: naphthalene), 5.47 (d, J = 5.3 Hz, 1H: glucose-3OH), 5.33 (m, 2H: —CH═CH—), 5.13 (d, J = 5.6 Hz, 1H: glucose-2OH), 4.96 (t, J = 9.1 Hz, 1H: glucose-1), 4.19 (m, 1H: glucose-6), 3.95 (m, 1H: glucose-4), 3.74–3.73 (m, 2H: glucose-5, 6), 3.53 (m, 1H: glucose-3), 3.27 (m, 1H: glucose-2), 2.18 (t, J = 7.3 Hz, 2H: —$COCH_2$—), 2.13 (m, 4H: —CH_2—), 1.49 (m, 4H: —CH_2—), 1.24 (m, 18H: —CH_2—), 0.86 (t, J = 6.5 Hz, 3H: —CH_3). ESI-MS (m/z): 596.38 $[M + OH]^-$. Anal. Calcd for $C_{34}H_{50}BNO_6$: C, 70.46; H, 8.70; N, 2.42. Found: C, 70.10; H, 8.79; N, 2.40.

Synthesis of Amphiphilic Monomer 2. 2-Naphthaleneboronic acid was purchased from Tokyo Chemical Co. and was used without purification. The synthesis and purification procedure of **2** was similar to that of **1** as described above. ^{1}H NMR (400 MHz, DMSO-d_6, δ): 8.38 (d, J = 9.1 Hz, 1H: NH), 8.34 (s, 1H: naphthalene), 7.95 (dd, J = 1.2 and 8.0 Hz, 1H: naphthalene), 7.92–7.86 (m, 2H: naphthalene), 7.82 (dd, J = 1.2 and 8.0 Hz, 1H: naphthalene), 7.57–7.50 (m, 2H: naphthalene), 5.46 (d, J = 4.9 Hz, 1H: glucose-3OH), 5.36–5.33 (m, 2H: —CH═CH—), 5.12 (d, J = 5.3 Hz, 1H: glucose-2OH), 4.96 (t, J = 9.1 Hz, 1H: glucose-1), 4.19 (dd, J = 4.9 and 10 Hz, 1H: glucose-6), 3.89 (td, J = 3.1 and 9.1 Hz, 1H: glucose-4), 3.68–3.65 (m, 2H: glucose-5, 6), 3.50 (ddd, J = 4.9, 7.3, and 9.1 Hz, 1H: glucose-3), 3.26 (ddd, J = 5.3, 7.3, and 9.1 Hz, 1H: glucose-2), 2.12 (t, J = 7.3 Hz, 2H: —$COCH_2$—), 1.99 (m, 4H: —CH_2—), 1.50 (m, 4H: —CH_2—), 1.25 (m, 18H: —CH_2—), 0.85 (t, J = 6.7 Hz, 3H: —CH_3). ESI-MS (m/z): 596.38 $[M + OH]^-$. Anal. Calcd for $C_{34}H_{50}BNO_6$: C, 70.46; H, 8.70; N, 2.42. Found: C, 70.19; H, 8.75; N, 2.41.

SEM Observation. The nanotube organogel was lyophilized, and then the resultant xerogel was dropped onto the grid. The nanotubes were observed by SEM (Carl Zeiss, FE-SEM Supra 40) at 1 kV equipped with a chamber SE detector (SE2 mode).

TEM Observation. The $CHCl_3$ dispersion of the nanotape or nanotube was dropped onto a carbon grid and dried by standing at room temperature. TEM (Hitachi, H-7000) was operated at 75 kV.

Powder XRD and IR Measurements. The obtained nanotape and nanotube were lyophilized and subjected to measure XRD at 25 °C with a Rigaku diffractometer (Type 4037) using graded *d*-space elliptical side-by-side multilayer optics, monochromated Cu Kα radiation (40 kV, 30 mA), and an imaging plate (R-Axis IV). IR spectra were measured with a Fourier transform IR spectrometer (JASCO FT-620)

dx.doi.org/10.1021/cm2030526 | *Chem. Mater.* 2012, 24, 209–214

and an attenuated total reflection (ATR) accessory system (Diamond MIRacle, horizontal ATR accessory with a diamond crystal prism, PIKE Technologies, USA).

Fluorescence Microscopic Observation. Fluorescence microscopic observation for the nanotube encapsulating anthracene in $CHCl_3$ was performed using an inverted microscope (Olympus IX71) equipped with a CCD camera (Hamamatsu ORCA-ER). Excitation optical source was prepared by a high pressure mercury lamp (100 W, Olympus BH2-REL-T3) and a fluorescence mirror unit (Olympus U-MGFPHQ: a 330−385 nm band-pass filter).

Spectroscopic Measurements. UV/vis and fluorescence spectra of the THF solutions of the amphiphilic monomers **1** and **2** and the $CHCl_3$ dispersed solution of nanotape, nanotube, and the nanotube encapsulating anthracene were measured at 25 °C using a U-3300 spectrophotometer (Hitachi) equipped with BU150A temperature control (YAMATO) and F-4500 spectrophotometer (Hitachi) equipped with DCI temperature control (HAAKE), respectively. The quantum yields of naphthalene (7.6×10^{-5} M in cyclohexane) and anthracene (1.0×10^{-5} M in ethanol) solutions were evaluated as standard samples. The calculated values, 0.23 at 270 nm for naphthalene and 0.27 at 355 nm for anthracene, were identical to the reported one within ±0.01. The $CHCl_3$ dispersed solution of the nanotube and nanotube encapsulating anthracene were excited by illumination with a UV-pulsed beam from an Nd:YAG laser (EXSPLA 2143B; third harmonic, 355 nm; pulse duration, 30 ps; beam diameter, 9 mm; repetition rate, 10 Hz; beam power, 1 mJ per pulse; not focused on the sample). All measurements were performed at room temperature (298 K) and repeated three times.

Encapsulation Method. Preparation of the nanotube encapsulating anthracene was performed by mixing a $CHCl_3$ solution of anthracene with the lyophilized nanotube. Capillary action enabled the nanotube to encapsulate anthracene into the nanochannel. After aging overnight, the solution was filtered through a polycarbonate membrane with 0.2 μm pore size. The residual nanotube was washed several times to remove anthracene outside of the nanotube. Complete destruction of the nanotube by dissolving in DMSO caused the release of the encapsulated anthracene to the bulk solution. The concentration of the released anthracene was determined by fluorescence spectroscopy. The calculated value was adopted as the concentration of the encapsulated anthracene (Supporting Information Figure S6).

To monitor the release behavior of the encapsulated anthracene from the nanochannel to bulk solution, the nanotube encapsulating anthracene was dispersed in $CHCl_3$ and then the solution was left to stand for 80 h. The release ratio was estimated to be a few percent even after 12 h (Supporting Information Figure S7), which scarcely influenced the energy transfer efficiency.

■ ASSOCIATED CONTENT

Supporting Information

Synthetic scheme, TEM and fluorescence microscopic images, XRD, IR, absorption and fluorescence spectra, and encapsulation and release profiles (Figures S1−S10; PDF). This material is available free of charge via the Internet at http://pubs.acs.org.

■ AUTHOR INFORMATION

Corresponding Author

*Fax: +81-29-861-4545; E-mail: n-kameta@aist.go.jp.

■ REFERENCES

(1) (a) Balaban, T. S.; Tamiaki, H.; Holzwarth, A. R. *Top. Curr. Chem.* **2005**, *258*, 1−38. (b) Psencik, J.; Ma, Y.-Z.; Arellano, J. B.; Hála, J.; Gillbro, T. *Biophys. J.* **2003**, *84*, 1161−1179. (c) Prokhorenko, V. I.; Holzwarth, A. R.; Müller, M. G.; Schaffner, K.; Miyatake, T.; Tamiaki, H. *J. Phys. Chem. B* **2002**, *106*, 5761−5768. (d) Prokhorenko, V. I.; Steensgard, D. B.; Holzwarth, A. R. *Biophys. J.* **2000**, *79*, 2105−2120.

(2) (a) Banerjee, S.; Das, R. K.; Maitra, U. *J. Mater. Chem.* **2009**, *19*, 6649−6687. (b) Tsuda, A. *Bull. Chem. Soc. Jpn.* **2009**, *82*, 11−28. (c) Elemans, J. A. A. W.; Hameren, R.; Nolte, R. J. M.; Rowan, A. E. *Adv. Mater.* **2006**, *18*, 1251−1266. (d) Yagai, S.; Higashi, M.; Karatsu, T.; Kitamura, A. *Chem. Commun.* **2006**, 1500−1502. (e) Hoeben, F. J. M.; Jonkheijm, P.; Meijer, E. W.; Schenning, A. P. H. J. *Chem. Rev.* **2005**, *105*, 1491−1546.

(3) (a) Vijayakumar, C.; Praveen, V. K.; Kartha, K. K.; Ajayaghosh, A. *Phys. Chem. Chem. Phys.* **2011**, *13*, 4942−4949. (b) Babu, S. S.; Kartha, K. K.; Ajayaghosh, A. *J. Phys. Chem. Lett.* **2010**, *1*, 3413−3424. (c) Vijayakumar, C.; Praveen, V. K.; Ajayaghosh, A. *Adv. Mater.* **2009**, *21*, 2059−2063. (d) Ajayaghosh, A.; Praveen, V. K.; Vijayakumar, C. *Chem. Soc. Rev.* **2008**, *37*, 109−122. (e) Ajayaghosh, A.; Praveen, V. K.; Vijayakumar, C.; George, S. *Angew. Chem., Int. Ed.* **2007**, *46*, 6260−6265. (f) Ajayaghosh, A.; Praveen, V. K.; Srinivasan, S.; Varghese, R. *Adv. Mater.* **2007**, *19*, 411−415. (g) Ajayaghosh, A.; Vijayakumar, C.; Praveen, V. K.; Babu, S. S.; Varghese, R. *J. Am. Chem. Soc.* **2006**, *128*, 7174−7175.

(4) (a) Giansante, C.; Raffy, G.; Schäfer, C.; Rahma, H.; Kao, M.-T.; Olive, A. G. L.; Guerzo, A. D. *J. Am. Chem. Soc.* **2011**, *133*, 316−325. (b) Olive, A. G. L.; Guerzo, A. D.; Schäfer, C.; Belin, C.; Raffy, G.; Giansante, C. *J. Phys. Chem. C* **2010**, *114*, 10410−10416. (c) Giansante, C.; Olive, A. G. L.; Schäfer, C.; Raffy, G.; Guerzo, A. D. *Anal. Bioanal. Chem.* **2010**, *396*, 125−131. (d) Guerzo, A. D.; Olive, A. G. L.; Reichwagen, J.; Hopf, H.; Desvergne, J. P. *J. Am. Chem. Soc.* **2005**, *127*, 17984−17985.

(5) (a) Zhang, X.; Rehm, S.; Safont-Sempere, M.; Würthner, F. *Nat. Chem.* **2009**, *1*, 623−629. (b) Zhang, X.; Chen, Z.; Würthner, F. *J. Am. Chem. Soc.* **2007**, *129*, 4886−4887. (c) Hoeben, F. J. M.; Shklyarevskiy, I. O.; Pouderoijen, M. J.; Engelkamp, H.; Schenning, A. P. H. J.; Christianen, P. C. M.; Maan, J. C.; Meijer, E. W. *Angew. Chem., Int. Ed.* **2006**, *45*, 1232−1236.

(6) (a) He, Y.; Yamamoto, Y.; Jin, W.; Fukushima, T.; Saeki, A.; Seki, S.; Ishii, N.; Aida, T. *Adv. Mater.* **2010**, *22*, 829. (b) Yamamoto, Y.; Zhang, G.; Jin, W.; Fukushima, T.; Ishii, N.; Saeki, A.; Seki, S.; Tagawa, S.; Minari, T.; Tsukagoshi, K.; Aida, T. *Proc. Natl. Acad. Sci. U.S.A.* **2009**, *106*, 21051−21056. (c) Yamamoto, Y.; Fukushima, T.; Saeki, A.; Seki, S.; Tagawa, S.; Ishii, N.; Aida, T. *J. Am. Chem. Soc.* **2007**, *129*, 9276−9277. (d) Yamamoto, Y.; Fukushima, T.; Suna, Y.; Ishii, N.; Saeki, A.; Seki, S.; Tagawa, S.; Taniguchi, M.; Kawai, T.; Aida, T. *Science* **2006**, *314*, 1761−1764. (e) Yamamoto, Y.; Fukushima, T.; Jin, W.; Kosaka, A.; Hara, T.; Nakamura, T.; Saeki, A.; Seki, S.; Tagawa, S.; Aida, T. *Adv. Mater.* **2006**, *18*, 1297−1300.

(7) (a) Shao, H.; Seifert, J.; Romano, N. C.; Gao, M.; Helmus, J. J.; Jaroniec, C. P.; Modarelli, D. A.; Parquette, J. R. *Angew. Chem., Int. Ed.* **2010**, *49*, 7688−7691. (b) Kim, H. J.; Kang, S. K.; Lee, Y. K.; Seok, C.; Lee, J. K.; Zin, W. C.; Lee, M. *Angew. Chem., Int. Ed.* **2010**, *49*, 8471−8475. (c) Medforth, D. J.; Wang, Z.; Martin, K. E.; Song, Y.; Jacobsen, J. l.; Shelnutt, J. A. *Chem. Commun.* **2009**, 7261−7277. (d) Röger, C.; Miloslavina, Y.; Brunner, D.; Holzwarth, A.; Würthner, F. *J. Am. Chem. Soc.* **2008**, *130*, 5929−5939. (e) Behanna, H. A.; Rajangam, K.; Stupp, S. I. *J. Am. Chem. Soc.* **2007**, *129*, 321−327. (f) Ajayaghosh, A.; Varghese, R.; Mahesh, S.; Praveen, V. K. *Angew. Chem., Int. Ed.* **2006**, *45*, 7729−7732. (g) Ashkenasy, N.; Horne, W. S.; Ghadiri, M. R. *Small* **2006**, *1*, 99−102. (h) Würthner, F. *Chem. Commun.* **2004**, 1564−1579.

(8) (a) Miller, R. A.; Stephanopoulos, N.; McFarland, J. M.; Rosko, A. S.; Geissler, P. L.; Francis, M. B. *J. Am. Chem. Soc.* **2010**, *132*, 6068−6074. (b) Miller, R. A.; Presley, A. D.; Francis, M. B. *J. Am. Chem. Soc.* **2007**, *129*, 3104−3109. (c) Endo, M.; Fujitsuka, M.; Majima, T. *Chem.—Eur. J.* **2007**, *13*, 8660−8666.

(9) (a) Escosura, A.; de la.; Janssen, P. G. A.; Schenning, A. P. H. J; Nolte, R. J. M.; Cornelissen, J. J. L. M. *Angew. Chem., Int. Ed.* **2010**, *49*, 5335−5338.

(10) (a) Kholkin, A.; Amdursky, N.; Bdikin, I.; Gazit, E.; Rosenman, G. *ACS Nano* **2010**, *4*, 610−614. (c) Amdursky, N.; Molotskill, M.; Aronov, D.; Alder-Abramovich, L.; Gazit, E.; Rosenman, G. *Nano Lett.* **2009**, *9*, 3111−3115. (d) Ryu, J.; Lim, S. Y.; Park, C. B. *Adv. Mater.* **2009**, *21*, 1577−1581.

(11) Shimizu, T.; Masuda, M.; Minamikawa, H. *Chem. Rev.* **2005**, *105*, 1401−1443.

(12) Review: (a) Shimizu, T. *J. Polym. Sci., Part A* **2008**, *46*, 2601−2611. (b) Shimizu, T. *Bull. Chem. Soc. Jpn.* **2008**, *81*, 1554−1566. (c) Shimizu, T. *J. Polym. Sci., Part A* **2006**, *44*, 5137−5152.
(13) Review: (a) Fujita, S.; Inagaki, S. *Chem. Mater.* **2008**, *20*, 891−908. (b) Review: Calzaferri, G.; Huber, S.; Maas, H.; Minkowski, C. *Angew. Chem., Int. Ed.* **2003**, *42*, 3732−3758.
(14) Review: Kameta, N.; Minamikawa, H.; Masuda, M. *Soft Matter* **2011**, *7*, 4539−4561.
(15) (a) Yui, H.; Minamikawa, H.; Danev, R.; Nagayama, K.; Kamiya, S.; Shimizu, T. *Langmuir* **2008**, *24*, 709−713. (b) Kamiya.; Minamikawa, H.; Jung, J. H.; Yang, B.; Masuda, M.; Shimizu, T. *Langmuir* **2005**, *21*, 743−750.
(16) (a) Yamada, N.; Okuyama, K.; Serizawa, T.; Kawasaki, M.; Oshima, S. *J. Chem. Soc. Perkin Trans. II* **1996**, *12*, 2707−2713. (b) Garti, N.; Sato, K. *Crystallization and Polymorphism of Fats and Fatty Acids*; Marcel Dekker: New York, 1988; pp 139−187.
(17) Martin, O.; Mendicuti, F.; Saiz, E.; Mattice, W. L. *J. Polym. Sci., Part B: Polym. Phys.* **1999**, *37*, 253−266.
(18) (a) Deans, R.; Kim, J.; Machacek, M. R.; Swager, T. M. *J. Am. Chem. Soc.* **2000**, *122*, 8565−8566. (b) Luo, J. D.; Xie, Z. L.; Lam, J. W. Y.; Cheng, L.; Chen, H. Y.; Qiu, C. F.; Kwok, H. S.; Zhan, X. W.; Liu, Y. Q.; Zhu, D. B.; Tang, B. Z. *Chem. Commun.* **2001**, 1740−1741.
(19) Nakashima, T.; Kimizuka, N. *Adv. Mater.* **2002**, *14*, 1113−1116.
(20) Inagaki, S.; Ohtani, O.; Goto, Y.; Okamoto, K.; Ikai, M.; Yamanaka, K.; Tani, T.; Okada, T. *Angew. Chem., Int. Ed.* **2009**, *48*, 4042−4046.
(21) (a) Kameta, N.; Masuda, M.; Minamikawa, H.; Mishima, Y.; Yamashita, I.; Shimizu, T. *Chem. Mater.* **2007**, *19*, 3553−3560. (b) Zhou, Y.; Shimizu, T. *Chem. Mater.* **2008**, *20*, 625−633. (c) Kameta, N.; Asakawa, M.; Masuda, M.; Shimizu, T. *Soft Matter* **2011**, *7*, 85−90.